



# Humidity effects on the detection of soluble and insoluble nanoparticles in butanol operated condensation particle counters

Christian Tauber<sup>1</sup>, Sophia Brilke<sup>1</sup>, Peter Josef Wlasits<sup>1</sup>, Paulus Salomon Bauer<sup>1</sup>, Gerald Köberl<sup>1</sup>, Gerhard Steiner<sup>1,2,3</sup>, and Paul Martin Winkler<sup>1</sup>

<sup>1</sup>Faculty of Physics, University of Vienna, Boltzmanngasse 5, 1090 Vienna, Austria

<sup>2</sup>Institute for Ion Physics and Applied Physics, University of Innsbruck, Technikerstraße 25/3, 6020 Innsbruck, Austria

<sup>3</sup>Grimm Aerosol Technik Ainring GmbH & Co Kg, Dorfstraße 9 Ainring, 83404 Ainring, Germany

**Correspondence:** Christian Tauber ([christian.tauber@univie.ac.at](mailto:christian.tauber@univie.ac.at))

**Abstract.** In this study the impact of humidity on heterogeneous nucleation of n-butanol onto hygroscopic and nonabsorbent particles was investigated using a fast expansion chamber and commercial continuous flow type condensation particle counters (CPCs). More specifically, we measured the activation probability of sodium chloride (NaCl) and silver (Ag) nano-particles by using n-butanol as condensing liquid with the size analyzing nuclei counter (SANC). In addition, the cut-off diameter of regular butanol based CPCs for both seed materials was measured and compared to SANC results. Our findings reveal a strong humidity dependence of NaCl particles in the sub-10 nm size range since the activation of sodium chloride seeds is enhanced with increasing relative humidity. For Ag seeds this humidity dependence was not observed, underlining the importance of molecular interactions between seed and vapor molecules. Consequently, the cut-off diameter of a butanol based CPC can be reduced significantly by increasing the relative humidity. This finding suggests that cut-off diameters of butanol CPCs under ambient conditions are likely smaller than corresponding cut-off diameters measured under clean (dry) laboratory conditions. At the same time, we caution that the humidity dependence may lead to wrong interpretations if the aerosol composition is not known.

## 1 Introduction

Aerosol particles are present in the atmosphere in various kinds. Since the size of these particles range from a few nanometers up to 100  $\mu\text{m}$  the detection method has to be carefully chosen. Typically, aerosol particles are measured in number concentration and mass concentration. The current state-of-the-art technology of real-time aerosol mass concentration measurements is based on acoustic and electromechanical sensors (Soysal et al., 2017). On the other hand, number concentration measurements are conducted using optical and electrical aerosol instruments. Ultrafine particles which have diameters less than 100nm are known to increase the risk of respiratory and cardiovascular diseases (Saghafifar et al., 2009; Kaiser, 2005; Pope et al., 2009). The mass contribution of ultrafine particles is small and therefore the number density of particles is suggested to be more related to adverse health effects (Nel, 2005). As a consequence, number concentration measurements are preferred in health-related studies, clean room technology, as well as in cloud formation and climate related studies (Saghafifar et al., 2009).



In the atmosphere nano-particle formation by gas-to-particle conversion has been observed in a variety of locations and conditions. On a global scale, it is seen as an important source controlling the number size distribution of atmospheric aerosols (Kulmala et al., 2014). Thereby, a phase transition from the gaseous to the liquid or solid state occurs in the presence of supersaturated vapors. This process is called nucleation and arises homogeneously from gas molecules only, or heterogeneously by the formation of vapor clusters on preexisting particles (Tauber et al., 2018). These nano-particles then can grow up to a size at which they act as a cloud condensation nuclei (CCN) (Spracklen et al., 2008; Merikanto et al., 2009). Thereby nanometer-sized particles contribute to the indirect radiative forcing, thus influencing the Earth's climate (IPCC, 2013).

Heterogeneous nucleation in the atmosphere takes place for seed particles and vapor molecules of different chemical composition. Aerosol particles acting as seeds in the heterogeneous nucleation process have different physicochemical surface properties such as charging state, wettability, shape or size. Interactions between the seed and the vapor molecules as well as solubility play an important role (Kupc et al., 2013; McGraw et al., 2012, 2017). Atmospheric aerosol can contain hygroscopic salts and is therefore sensitive to relative humidity which can contribute to a phase transition within the aerosol particle.

A highly hygroscopic example is sodium chloride (NaCl) which mainly originates from sea spray. Water vapor strongly influences the phase of the hygroscopic NaCl particles which under dry conditions exhibit a solid crystalline structure. At high relative humidity (RH), salt particles take up water and form a saline droplet with increased volume which affects its physical, chemical and optical properties. In contrast to increasing RH, aqueous saline aerosol particles shrink with decreasing relative humidity. Thereby the water evaporates and the seed crystalizes (Martin, 2000; Biskos et al., 2006).

In the atmosphere usually more than a single species of vapor molecules contributes to the vapor-liquid nucleation. Both processes, gas-to-particle conversion and the existence of insoluble particles in the atmosphere, can initiate heterogeneous nucleation processes (Wang et al., 2013). One commonly used technique to measure preexisting particles in the atmosphere are Condensation Particle Counters (CPCs), which are oftentimes using n-butanol as working fluid (McMurry, 2000). However, under ambient conditions significant amounts of water vapor usually enter the CPC and can modify the detection behaviour of the CPC. Previous studies on binary heterogeneous nucleation of n-propanol-water vapor mixtures on sodium chloride (NaCl) particles indicated a decrease of the activation barrier and reported a soluble-insoluble transition in the particle activation behaviour (Petersen et al., 2001). Butanol is chemically similar to propanol and therefore the process of heterogeneous nucleation of n-butanol and water vapor on nanometer sized particles is of high relevance in ambient nanoparticle characterization studies.

Over the last years various studies investigated the onset saturation ratio and the nucleation temperature for different seeds and vapors. These studies include measurements by Chen and Tao (2000) for water on SiO<sub>2</sub> and TiO<sub>2</sub>, and Schobesberger et al. (2010) for n-propanol on silver (Ag) and sodium chloride seeds. All studies show that the expected temperature trend agrees with theory, except for the nucleation of n-propanol on NaCl particles. In this specific case a reversed temperature trend of the onset saturation ratio compared to the Kelvin equation in the temperature range from 262 K to 287 K was recorded (Schobesberger et al., 2010). Despite the common use of butanol as working fluid for the detection of ambient nanoparticles surprisingly little nucleation research has been done in the sub-10 nm size range. Here we investigate heterogeneous nucleation of n-butanol vapor on differently sized seeds depending on relative humidity, charge state and nucleation temperature. We aim at getting a better understanding of the effect of RH on the nucleation process in CPCs with the focus on sub-5 nanometer



particles. Thereby the relative humidity effect on the lower particle detection limit can be analyzed. The results help to improve the understanding of heterogeneous nucleation of n-butanol vapor on soluble and insoluble seeds. By that the acting mechanism during the nucleation process can be analyzed and used to explain changes of the counting efficiencies in commercial CPCs (Ankilov et al., 2002).

## 5 2 Experimental Section

We examined the nucleation probability and counting efficiency of n-butanol based CPCs as shown schematically in Figure 1. Ag and NaCl particles were generated in a tube furnace (Scheibel and Porstendörfer, 1983) which was supplied with synthetic air (ALPHAGAZ 1 AIR,  $\geq 99.999\%$  (5.0), Air Liquide) or particle-free dry compressed air. The flow carrying the polydisperse aerosol was kept constant at 3 L/min through the Americium 241 (Am-241) charger and the nano differential mobility analyzer (nDMA) for both experimental approaches. By applying positive or negative voltage to the nDMA a monodisperse negatively or positively charged particle fraction was selected. By placing an Am-241 charger either at the Size Analyzing Nuclei Counter (SANC) or the CPC inlet the size selected particles were neutralized. Subsequently, ions that form inside the charger were removed using an ion trap. An adjustable well-defined flow of humid air joined the aerosol flow after the nDMA in order to vary the humidity of the CPC inlet flow. Two humidity sensors (HIH-4000-004, Honeywell) monitored the humidity of the aerosol flow before and after the injection of the humid flow. The amount of water vapor during the counting efficiency measurements was kept constant.

Measurements of heterogeneous nucleation of n-butanol at nucleation temperatures ranging from 270 K to 292 K were carried out with the SANC (Wagner et al., 2003). To this end, monodisperse particle fractions were mixed with a carrier gas flow of 5 L/min containing n-butanol vapor and led into the expansion chamber of the SANC. N-butanol vapor was added to the system by controlled injection using a syringe pump, followed by quantitative evaporation of the liquid beam in a heating unit (Winkler et al., 2008). As a result, the well-defined and nearly saturated binary vapor-air mixture together with size selected, neutralized monodisperse seed particles from the nDMA was passed into the temperature controlled expansion chamber. Vapor supersaturation was achieved by adiabatic expansion and the number concentration of droplets nucleating on the seeds was measured with the Constant Angle Mie Scattering (CAMS) method (Wagner, 1985). Based on the CAMS-method a one to one correlation between the time dependent measured scattered light flux under a constant angle and the calculated scattered light flux as a function of droplet size can be established. Thus, we are able to determine the growth curve of the growing droplets which can be compared to theoretical calculations from a condensation model. Thereby, the saturation ratio can be verified with an accuracy of 2-3 percent. Thus, the radius and the number concentration of the growing droplets could be determined simultaneously. By varying the chamber temperature and the pressure drop in the expansion chamber, different nucleation conditions were analyzed. The nucleation or activation probabilities were measured with the SANC/CAMS method (Wagner et al., 2003). To evaluate the onset saturation ratio, which corresponds to a nucleation probability value of  $P = 0.5$ , the experimental data were fitted with a two-parameter fit function (Winkler et al., 2016).

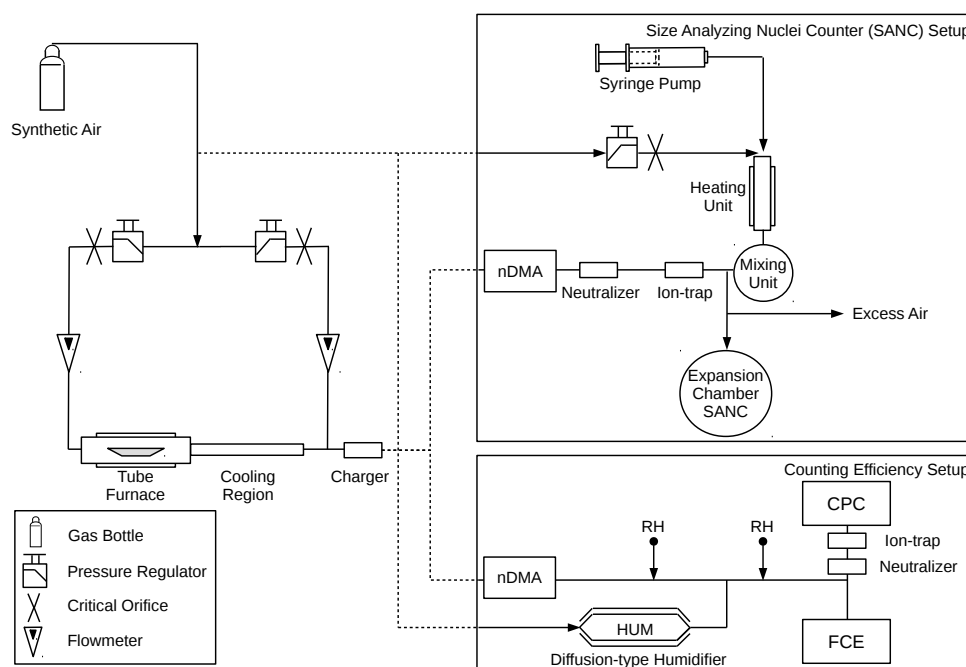


**Figure 1.** The experimental setup for evaluating the supersaturation and nucleation temperature with the SANC and the relative humidity dependent counting efficiency measurements of a continuous flow type CPC (TSI 3776 UCPC), which was measured by operating a Faraday Cup Electrometer (FCE) in parallel.

In addition to the SANC measurements, the counting efficiencies of three ultrafine continuous flow CPCs (Model UCPC 3776, TSI Inc., Minneapolis, USA), which temperature settings were changed over a range of 18 degrees, were measured. In contrast to the SANC, the supersaturation is obtained by saturating a laminar flow and subsequently cooling the aerosol together with the saturated flow in the condenser. Both methods lead to heterogeneous nucleation and condensation of n-butanol vapor on the aerosol particles due to a temperature decrease. Thereby the particles grow to a size at which they can be detected optically. To measure the detection efficiency of the TSI UCPCs the aerosol flow subsequent to size classification was symmetrically split. The aerosol was passed to three CPCs ( $N_{CPC,1-3}$ ) each operating at different temperature settings (see Table 1), and to the Faraday Cup Electrometer (FCE) ( $N_{FCE}$ ), which was operated in parallel. Thereby the counting efficiency was determined relative to a FCE (Model 3068B Aerosol Electrometer, TSI Inc., Minneapolis, USA). Hence the detection efficiency  $\eta$  of a UCPC can be determined by comparing the number concentration of the CPC  $N_{CPC,1-3}$  and the total number concentration  $N_{FCE}$  as follows:

$$\eta = \frac{N_{CPC,1-3}}{N_{FCE}}. \quad (1)$$



**Table 1.** Temperature settings of the three TSI 3776 UCPCs used in this study in parallel.

settings	low T [ °C ]	standard T [ °C ]	high T [ °C ]
condenser	1.1	10.0	18.9
saturator	30.1	39.0	47.9
optics	31.1	40.0	48.9

By operating the CPCs at different temperature settings we were able to analyze the detection efficiency with various peak super saturation ratios (Tauber et al., 2019). The particle detection efficiency mainly depends on the activation probability which is primarily a function of supersaturation and particle diameter (Barmounis et al., 2018). By conducting detection efficiency measurements the cut-off diameter is determined, which represents the mobility diameter where 50% of the particles can be counted in a CPC.

### 3 Results and Discussion

#### 3.1 Temperature and Humidity Effects

Here we report measurements of the onset saturation ratio of n-butanol depending on nucleation temperature and humidity with the SANC. The heterogeneous nucleation probability ( $P$ ) for different seeds and seed properties in the size range of 2.5 to 10.5 nm mobility diameter was investigated. The heterogeneous nucleation probability represents the number concentration of activated seeds normalized to the total number concentration of the aerosol. It depends on the saturation ratio which is given by the ratio of partial vapor pressure divided by the equilibrium vapor pressure at the corresponding temperature after expansion (nucleation temperature  $T_{nuc}$ ). Measurements were conducted at constant  $T_{nuc}$  by varying the vapor amount and keeping the pressure drop constant. In a recent study we have shown that with reduced nucleation temperatures the onset saturation ratio needed to activate a certain Ag particle size increases (Tauber et al., 2019). This is in line with classic Kelvin predictions (Thomson, 1871). To investigate the impact of RH on heterogeneous nucleation probability the Ag measurements were complemented by NaCl seeds. The resulting onset saturation ratios depending on the nucleation temperatures are shown in Figure 2. Heterogeneous nucleation of n-butanol vapor on NaCl and Ag aerosol particles shows a remarkably different behavior. An inverse temperature trend for NaCl seeds was identified when compared to the Kelvin prediction, except for the smallest sodium chloride particles with a mobility diameter of 2.5 nm. Such a trend was not found for silver nano-particles.

This finding is consistent with already published results from Schobesberger et al. (2010) for n-propanol, where an inversed temperature trend for NaCl but not for Ag seeds could be observed. To rule out any humidity effects, the sheath air of the nDMA was monitored with a commercial relative humidity sensor during the measurements. Thereby an accumulation of water in the used silica gel dryer of the sheath air loop could be recorded. The water aggregation in the drier originating from the compressed air supply reached values up to 10% RH at 22°C room temperature. As a consequence, the carrier gas

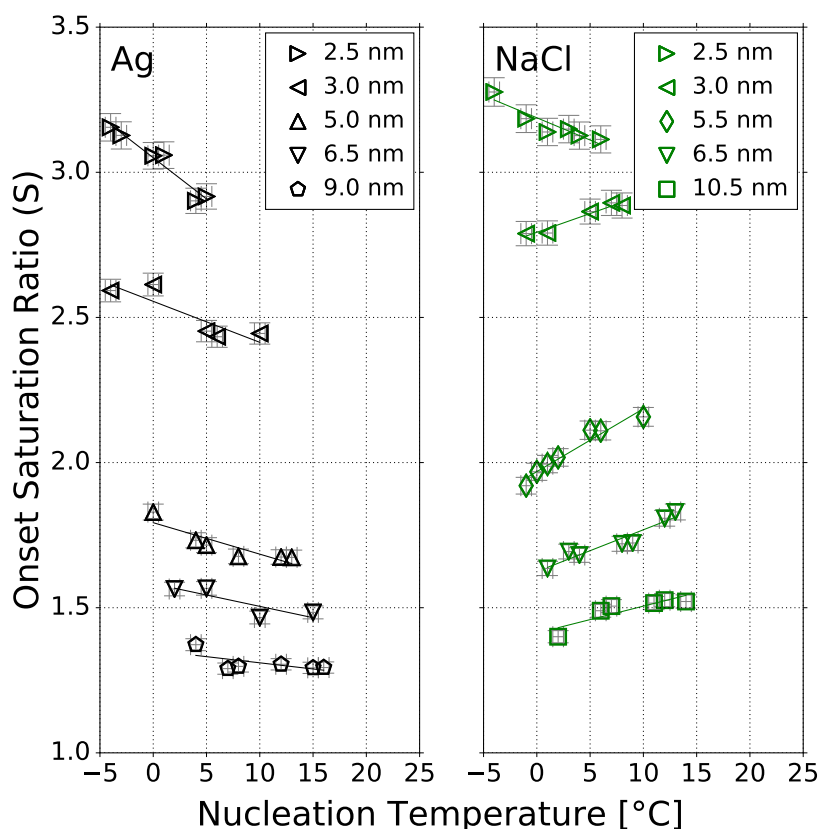


**Figure 2.** The onset saturation ratio versus nucleation temperature for neutral Ag (black) and NaCl (green) particles of different mobility equivalent diameters. With decreasing temperature the onset saturation ratio decreases for sodium chloride and increases for silver nanometer sized particles. Only the 2.5 nm NaCl seeds do not follow the inverse temperature trend. Lines represent a linear fit of data to show the temperature dependence for NaCl and Ag seeds. The onset saturation ratio increases with decreasing seed size for both test aerosols.

supplement for the experiment was changed from dried and filtered compressed air to synthetic air and additional measurements were performed with a relative humidity  $< 2.5\%$ .

The experimental values are shown in Figure 3 for neutral sodium chloride seeds and listed in Table S5-S9 of the supporting information for both considered aerosol species. The needed onset saturation ratio for activating "dry particles" of a certain size is at the same value as for "high" RH values ( $< 10\%$ ) or (with one exception) increased for dry measurements (RH  $< 2.5\%$ ). In other words, the additional small amount of water vapor during the measurements decreases the energy barrier which has to be overcome to activate a sodium chloride nano-particle with n-butanol in the observed size range. This finding suggests that already small contaminations of water vapor can influence the heterogeneous nucleation of butanol which agrees with already published studies for n-propanol-water mixtures on Ag and NaCl particles (Wagner et al., 2003).

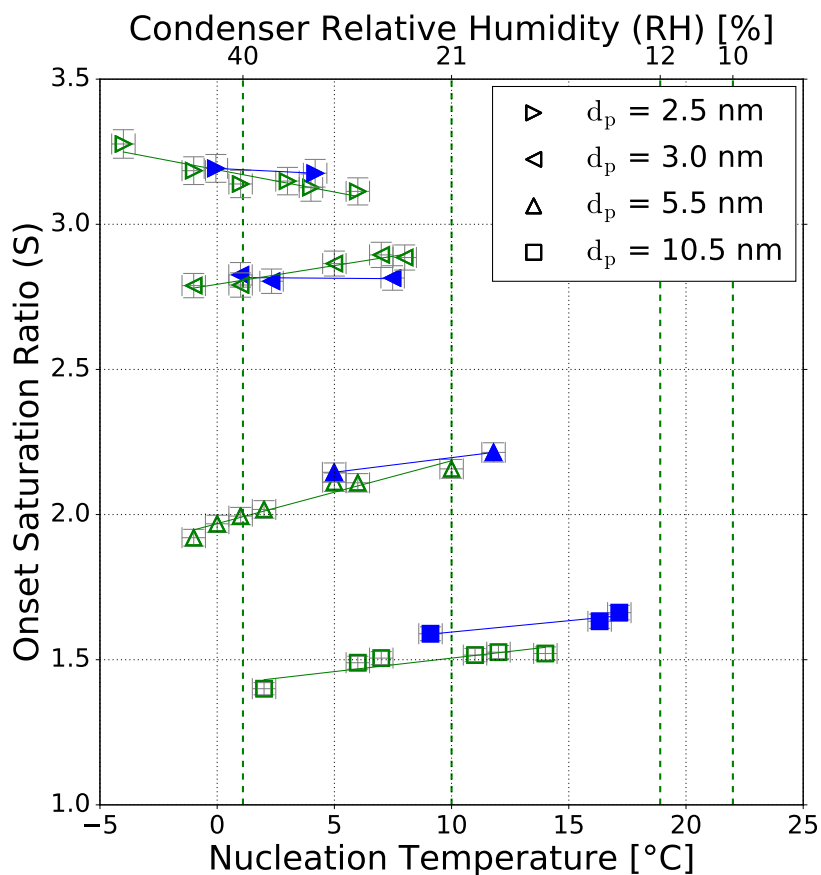


**Figure 3.** The onset saturation ratio versus nucleation temperature for NaCl particles of different mobility equivalent diameter. The green symbols show the onset saturation values recorded with relative humidity values  $\leq 10\%$  and the blue symbols represent measurement values when the RH was  $< 2.5\%$ . The green dashed vertical lines represent the calculated relative humidities at the corresponding preset condenser temperature (see Table 1) with a starting value of 10% RH at 22°C. The increased relative humidity inside the condenser of a TSI 3776 UCPC for reduced nucleation temperatures is shown which will be discussed in the counting efficiency measurements section.

For the heterogeneous nucleation of n-butanol on silver seeds no decreased onset saturation ratio was observed during the presence of water vapor. The inverse temperature dependence for NaCl and synthetic air as carrier gas (blue symbols in Figure 3) vanishes for small mobility diameters ( $< 3.5$  nm), but particle sizes above 3.5 nm still follow the unusual temperature dependence. This indicates that sodium chloride particles act differently in the observed size range. It seems that NaCl seeds at sizes below  $\sim 3.5$  nm are less prone to dissolution or restructuring effects. As a result the nucleation of n-butanol on small NaCl seeds is comparable to silver clusters and the inverse temperature trend vanishes and follows the Kelvin relation. One other remaining question is whether the charge sign during mobility selection has an effect on the heterogeneous nucleation.



**Table 2.** SANC experimental results for the onset saturation ratio for neutral (n), positively (+) and negatively (-) charged particles.  $D_p$  is the mean mobility equivalent diameter,  $\sigma_g$  the mean geometric standard deviation and  $S_{onset}$  the onset saturation ratio.

$D_p$ [nm]	$\sigma_g$	Ag ( $RH < 2.5\%$ )			NaCl ( $RH < 2.5\%$ )		
		$S_{onset}$	$S_{onset}$	$S_{onset}$	$S_{onset}$	$S_{onset}$	$S_{onset}$
		n	+	-	n	+	-
2.5	1.073	3.10	3.07	-	3.19	3.20	3.04
3.0	1.070	2.48	2.48	-	2.81	2.72	2.64
3.5	1.067	2.33	2.33	-	2.60	2.54	2.47
5.5	1.065	1.85	1.85	1.83	2.21	-	2.20
9.0	1.068	1.34	1.36	-	-	-	-
10.5	1.067	-	-	-	1.64	1.66	1.63

Therefore additional measurements focusing on charge and humidity for NaCl particles in the corresponding nanometer range were conducted.

### 3.2 The Influence of Charge and Particle Restructuring Effects

To investigate the charge effect on heterogeneous nucleation of n-butanol vapor on silver and sodium chloride particles the neutralizer and ion-trap in front of the expansion chamber (see Figure 1) were removed. Thereby the seeds were positively or negatively charged depending on the applied voltage to the nDMA. Nucleation studies were conducted with constant nucleation temperatures but varying charge state of the aerosol with synthetic air as carrier gas. For positively charged silver particles no charge dependence on heterogeneous nucleation was found. However, NaCl seeds show a charge enhancement, especially below 5 nm. As listed in Table 2 the necessary onset saturation ratio for neutral and positively charged silver particles is below the NaCl values and no charge enhancement was found. Negatively charged Ag particles could not be fully investigated due to technical problems with the SANC at the end of the measurement run. Kangasluoma et al. (2016) conducted measurements using tungsten oxide, ammonium sulfate and tetraheptylammonium bromide nano clusters of different charge states to determine the counting efficiency. During their studies a charge enhancement of particle activation was observed similar to our findings regarding the NaCl measurements.

It is known from prior research that NaCl aerosol particles, which are generated by evaporation and condensation in a tube furnace, undergo a structural change in the presence of water (Krämer et al., 2000; Biskos et al., 2006) or n-propanol (Petersen et al., 2001; Kulmala et al., 2001). As a consequence the particles shrink in the presence of polar vapors. This shrinkage was also investigated in our study for n-butanol and water and the experimental results for water are shown in Figure 4. We measured monodisperse NaCl aerosols with mobility diameters between 4.5 and 11 nm at relative humidities up to 50%. However, with decreasing mobility diameter also the shrinkage becomes less. For example, an 11 nm NaCl particle exposed to 40% RH is shrinking by about 15% and a 4.5 nm particle at 40% RH shrinks only by about 3%. Hence the structural rearrangement for particles below 5 nm is not as pronounced as for larger ones. This decrease in size for particles > 5 nm is a

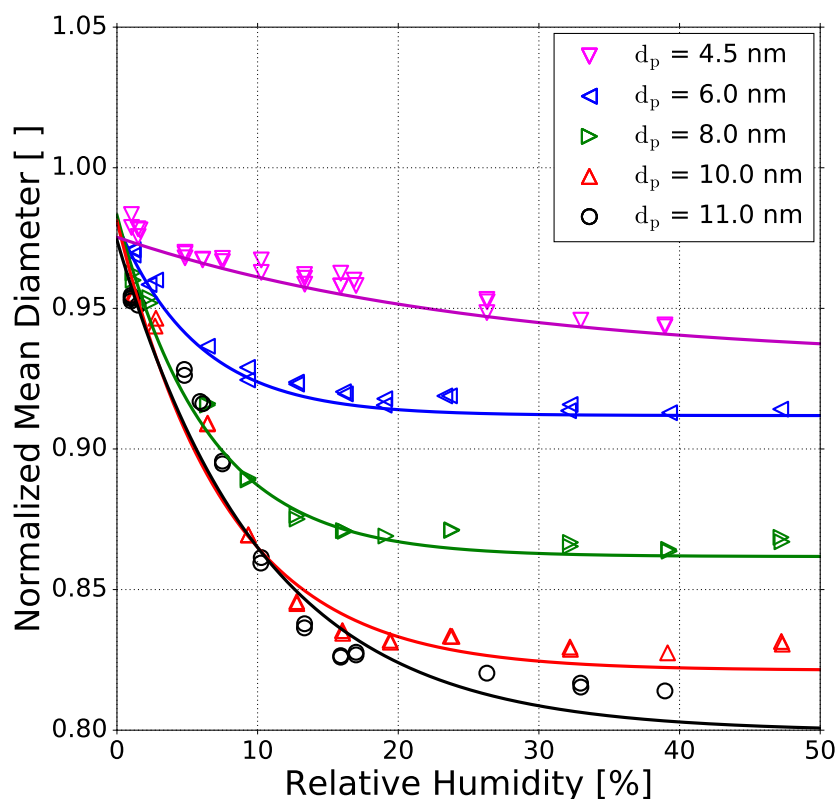


**Figure 4.** Normalized mean diameter of sodium chloride particles as a function of relative humidity which represents the shrinkage of NaCl seeds in the presence of water vapor. All sizes are mobility equivalent diameters. Each line represents a tentative three-parameter fit of an exponential decay.

result of solvation on the surface of the NaCl particle caused by the presence of water vapor and thereby a wet surface accrues (Castarède and Thomson, 2018). Due to this dissociation process and the resulting liquid surface the particle attracts more polar vapor molecules. In addition the overall polarity of the working fluid of n-butanol and water mixture increases, due to the higher dipole moment of water ( $6.2 \times 10^{-30}$  Cm) compared to n-butanol ( $5.8 \times 10^{-30}$  Cm) (Reichardt and Welton, 2011).  
5 As a result, additional vapor molecules can more readily condense onto the seed aerosol. This mechanism could explain the resulting lower onset saturation ratio needed for NaCl seeds  $\geq 3$  nm as shown in Figure 3 for lower nucleation temperatures. As a consequence, by reducing the nucleation temperature the saturation vapor pressure decreases leading to an increase in the saturation ratio for water (RH is increasing, see Figure 3, upper x-axis).

In summary, the SANC measurements allowed us to study the heterogeneous nucleation of n-butanol depending on the  
10 charge state, nucleation temperature and humidity of the carrier gas. Charge enhanced nucleation could be found for sodium



**Table 3.** Calculated maxima of the CPC saturation ratio profiles  $S_{max}$  for low, standard and high temperature settings (Tauber et al., 2019), in comparison to the extrapolated  $S_{onset}$  as measured by the SANC.

$d_p$ [nm]		NaCl neutral ( $RH < 2.5\%$ )				NaCl neutral ( $RH < 10.0\%$ )			
		2.5	3.0	3.5	5.5	2.5	3.0	3.5	5.5
T settings	$S_{max}$	$S_{onset}$	$S_{onset}$	$S_{onset}$	$S_{onset}$	$S_{onset}$	$S_{onset}$	$S_{onset}$	$S_{onset}$
low	4.3	3.18	2.81	2.65	2.10	3.17	2.80	-	1.99
standard	3.4	3.15	2.81	2.57	2.20	3.03	2.92	-	2.18
high	2.8	3.11	2.80	2.50	2.28	2.90	3.03	-	2.37

chloride particles  $\leq 3.5$  nm, yet not for silver particles. By taking special care of the water vapor amount a humidity enhanced nucleation for sodium chloride seeds was found. Under dry conditions the observed inverse temperature trend for NaCl seeds  $< 3.5$  nm vanishes. For larger sodium chloride particles this trend is found to be persistent.

### 3.3 Counting Efficiency Measurements

5 In addition, counting efficiency measurements at variable condenser temperatures, but constant  $\Delta T$  between saturator and condenser, for a commercial n-butanol TSI 3776 UCPC, were performed. As a consequence, we were able to increase or decrease the saturation ratio profile as described by Tauber et al. (2019). The onset saturation ratio and nucleation temperature measured with the SANC for a classified monodisperse seed particle could be compared to the three different temperature settings of the condenser. The maximum value for the calculated saturation ratio profiles and the extrapolated  $S_{onset}$  for NaCl  
 10 (partly extrapolated from the lines in Figure 2 and 3) under different humidity conditions at low, standard and high condenser temperatures are listed in Table 3. Thereby the ability to activate sodium chloride seeds in the cutoff range of a commercial UCPC could be analyzed. With increasing temperature the maximum saturation ratio ( $S$ ) decreases. As a result, the detection efficiency is shifting to bigger particle sizes as shown in Figure 5.

For the verification of our findings we measured the cut-off diameter, charge and relative humidity dependence for the TSI  
 15 3776 UCPC at different temperature settings. By varying the temperature settings of the UCPC we were also able to measure under different condenser temperatures (see Table 1). For comparison, particle classification with the nDMA was always performed under dry conditions ( $RH < 2.5\%$ ), so that the structural change of the sodium chloride clusters does not influence the classification and the size of the generated aerosol. After the size selection the particles were mixed with humidified air to reach RH values ranging from 0 to 40% as shown in Figure 1. Hence we were able to vary the relative humidity with an accuracy  
 20 of  $\pm 2.5\%$  by measuring the humidity before and after the mixing zone. Results of earlier studies indicated a discrepancy in the humidity dependence for sodium chloride and silver nano-particles on the detection efficiency of commercial CPCs (Sem, 2002). In the study conducted by Sem (2002), at increased RH the used CPCs had a lower cut-off diameter above 5 nm. In this size range the particle shrinkage plays an important role, the already mentioned emerging liquid surface would attract further vapor molecules. Consequently, the NaCl particles can be easier activated than an insoluble seed.

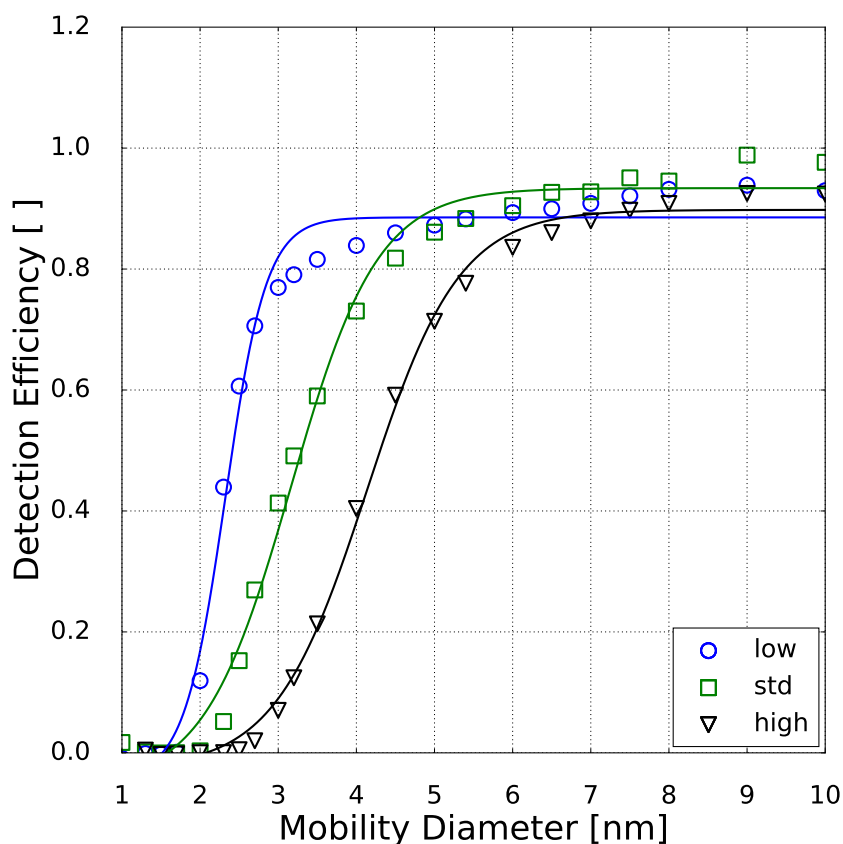


**Figure 5.** Detection efficiency as a function of mobility diameter for neutral sodium chloride particles. The symbols represent the measured counting efficiencies for low (circles), standard (std, squares) and high temperature (triangles) settings at 10% RH. The line displays a fit to the measured counting efficiencies (Wiedensohler et al., 1997). Thereby the corresponding cut-off diameter with the detection efficiency of 0.5 can be evaluated.

However, in this study a TSI 3776 UCPC was used which has a cut-off diameter well below 5 nm. An example detection efficiency measurement for the three CPC temperature settings is depicted in Figure 5. These measurements were conducted under elevated humidity conditions ( $RH = 10\%$ ), which leads to a decrease of the necessary onset saturation ratio for neutral NaCl seeds as shown in Figure 3. Due to the temperature decrease in the condenser the saturation ratio for water vapor increases up to  $S = 1.6$ . Studies conducted by Petersen et al. (2001) on binary heterogeneous nucleation of water-n-propanol vapor mixtures onto NaCl seeds also show that small amounts of water reduce the propanol activity substantially. Butanol is hardly miscible with water in macroscopic mixtures but still small amounts support the nucleation. The resulting cut-off diameters for neutral, negatively and positively charged sodium chloride nano-particles are shown in Figure 6. It can be clearly seen that with increasing relative humidity the cut-off diameter is decreasing for an UCPC operating at standard conditions (green)



from about 3.7 to about 2.0 nm for neutral NaCl clusters. To investigate the charge history of neutral particles, positively and negatively charged particles were neutralized. The resulting cut-off diameters are shown in Figure 6 (left). For sodium chloride no difference in nucleation due to the charge history could be found. Only under high n-butanol saturation ratio and high relative humidity conditions the previously negatively charged particles exhibit a lower cut-off diameter. In Figure 6 (right panel) the cut-off diameters as a function of RH are shown for particles of different polarity. Remarkably, for charged NaCl particles we find increased cut-off diameters compared to the neutral particles. Since the flow carrying the monodisperse aerosol and the flow of humid air are joined together in front of the CPC inlet, the increase of cut-off diameters could be a result of the increased attraction of charged NaCl particles to the water vapor under sub-saturated conditions. Thereby the  $Na^+$  and  $Cl^-$  ions get separated and form a solvent cage around themselves (Castarède and Thomson, 2018). This reduces the tendency of ions to aggregate (Loudon, 2009).

Li and Christopher J. Hogan (2017) performed measurements on the uptake of organic vapor molecules by nanometer scaled sodium chloride cluster ions using a DMA coupled to a Time-of-Flight (TOF) mass spectrometer. The results show that the polarity and the molecular structure of the vapor molecules control the vapor uptake. This is in agreement with our findings: The increased amount of water vapor improves the activation of sodium chloride clusters and the overall polarity of water and n-butanol vapor increases. In contrast to the SANC measurements no significant sign preference for charge enhanced nucleation could be found. This is probably due to the cut-off diameter size which is for most of the particles  $> 3$  nm. Except for negatively charged NaCl particles which show a charge enhancement as it was observed with the SANC for particles  $< 3$  nm mobility diameter. In addition, the recorded cut-off diameter for high T settings is in the size range where the inverse temperature trend was recorded by the SANC measurements. As a result, by decreasing the temperature the needed saturation ratio to activate a NaCl particle in this size range is decreasing. Furthermore, the increasing RH supports the structural rearrangement which influences the cut-off diameter (see Figure 6). As a matter of fact our results lead to an improved detection efficiency for sodium chloride clusters. At high relative humidity and low temperature settings the detection efficiency is further promoted by charge enhanced nucleation.

Results on the cut-off diameter depending on the relative humidity at the UCPC inlet for neutralized and charged silver seeds are shown in Figure 7. For Ag particles no shrinkage in mobility diameter could be measured and the clusters at a certain size can be assumed to be spherical (Winkler et al., 2016). As we can see in Figure 7 no relative humidity dependence on the cut-off diameter within the uncertainty range was observed. However, at reduced supersaturation (black) the cut-off diameter is lower for charged Ag nanoparticles. This indicates a charge enhanced nucleation for silver aerosol particles in the measured size range. Under highly supersaturated conditions (blue) and also at standard settings (green) the charge enhanced nucleation can be neglected. Thereby the particle charge only supports the nucleation and growth process under high n-butanol and water (black) saturation vapor pressure conditions. According to the SANC measurements no charge enhanced nucleation for positively charged Ag particles could be observed. The results agree well with the SANC measurements except for positively and negatively charged Ag seeds under high T settings (see Figure 7 (right panel)).

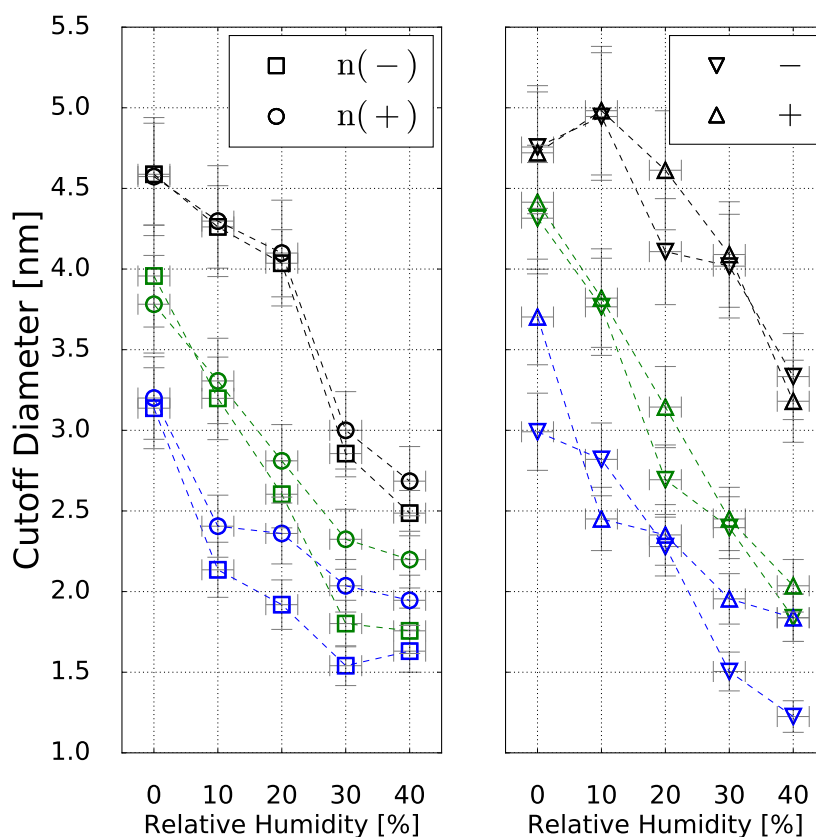


**Figure 6.** Cut-off diameter as a function of RH for neutral (left) and charged (right) sodium chloride seeds for low (blue), standard (green) and high (black) temperature settings.

#### 4 Conclusions

The presented measurements conducted with expansion and continuous flow type CPCs have shown that sodium chloride particles with a mobility diameter below 10 nm indicate different activation regimes. Under dry conditions for particles  $\leq 3$  nm no inverse temperature trend compared to classical Kelvin predictions was observed, however, for negatively charged seeds a charge enhanced activation was measured. Above 3.5 nm the charge does not play a role during the nucleation process. However, with increasing humidity the activation of NaCl particles can be enhanced. For Ag this humidity dependence could not be observed, which is an indicator for the importance of molecular interactions between the seed and the vapor molecules.

A recent study on heterogeneous nucleation of n-butanol on monoatomic ions has shown that charge dependence for the critical cluster does not favor a certain polarity (Tauber et al., 2018). However, under sub-saturated conditions the charging state of the ions plays an important role during the vapor uptake. Here the NaCl particles are in contact with the vapor molecules

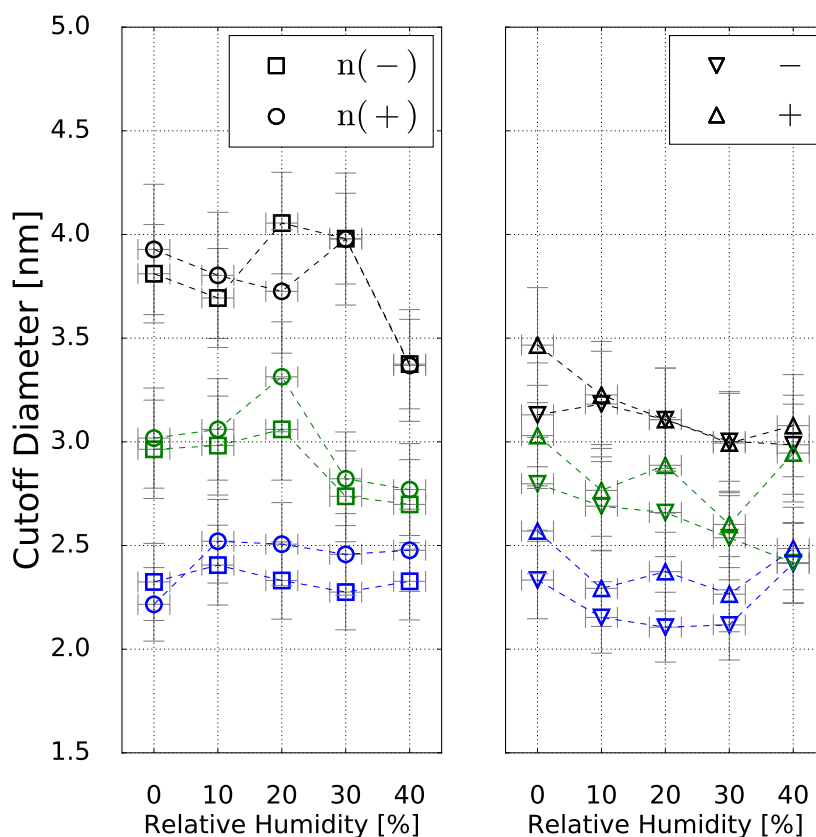


**Figure 7.** Cut-off diameter as a function of RH for neutral (left) and charged (right) Ag seeds for low (blue), standard (green) and high (black) temperature settings.

under sub-saturated conditions before the temperature drops and can already attach to the seeds. We performed measurements with NaCl seeds which are known to be hygroscopic. Therefore the water molecules dissociate the NaCl cluster and a solvation process takes place. As a result, the charged sodium chloride seeds attract the vapor molecules stronger and thereby the nucleation and condensational growth can start at smaller seed sizes.

- 5 As described by Li and Christopher J. Hogan (2017), the impact of vapor polarity in the measured particle size range, where interactions between single atoms are of importance, cannot be neglected. Additional water molecules increase the dipole moment of the n-butanol/water mixture and can change the structure of the sodium chloride cluster. Thereby charge effects on the surface support the initial steps of nucleation which then can lead to condensational growth. As a result, the energy barrier for activating nanometer sized NaCl particles can be reduced - this is comparable to already published results for n-propanol/water
- 10 mixtures conducted by Petersen et al. (2001). Our data show a strong effect of RH on heterogeneous nucleation of n-butanol on NaCl particles, but not for Ag seeds. This finding suggests that the different RH sensitivity is less a consequence of binary



heterogeneous nucleation but rather attributable to changing seed properties in the interaction with vapor molecules. According to the NaCl shrinkage measurements a change in diameter during the presence of water vapor - which we associated with a restructural effect - could be observed.

To improve our understanding of the observed restructuring effect future studies on heterogeneous nucleation depending on  
5 different seeds and humidity should be conducted. Also the herein presented measurements could be extended with the size selection after the particle restructuring. In particular the humidity dependent activation of hygroscopic nanoparticles which are present in the atmosphere would be of great interest. Thereby, the molecular interactions between the seed and the vapor molecules can be further evaluated which may lead to a model description.

Our results suggest that atmospheric measurements of ambient nanoparticles should take into account possible RH effects  
10 on the instrument's cut-off diameter when a large hygroscopic particle fraction is present. As a standard procedure, in many atmospheric studies the CPC inlet flow is dried before entering the instrument. We suggest that additional monitoring of the RH of the inlet flow is critical since the variation in RH between 0 and 40 % even shows a pronounced shift in the cut-off diameter. Thereby more particles of the nucleation mode are measured. In ambient conditions this mode usually contains high number concentrations of particles. Comparison between measurements taken in different regions with varying hygroscopic  
15 nanoparticle concentrations thus need to be treated with care to avoid wrong interpretation.

*Data availability.* Supplementary data associated with this article can be found in the online version.

*Author contributions.* Christian Tauber designed the setup, Christian Tauber performed the SANC experiments, Christian Tauber, Sophia Brilke and Peter Josef Wlasits performed the detection efficiency measurements, Paulus Salomon Bauer and Gerald Köberl performed the shrinkage measurements, Christian Tauber, Sophia Brilke, Peter Josef Wlasits, Gerhard Steiner and Paul Martin Winkler were involved in  
20 the scientific interpretation and discussion, and Christian Tauber, Sophia Brilke, Peter Josef Wlasits and Paul Martin Winkler wrote the manuscript.

*Competing interests.* The authors declare that they have no conflict of interest.

*Acknowledgements.* This work was supported by the European Research Council under the European Community's Seventh Framework Programme (FP7/2007/2013)/ERC grant agreement no. 616075. Dimitri Castarède and Lennart Graewe are thanked for helpful discussions.



## References

- Ankilov, A., Baklanov, A., Colhoun, M., Enderle, K.-H., Gras, J., Julanov, Y., Kaller, D., Lindner, A., Lushnikov, A., Mavliev, R., McGovern, F., O'Connor, T., Podzimek, J., Preining, O., Reischl, G., Rudolf, R., Sem, G., Szymanski, W., Vrtala, A., Wagner, P., Winklmayr, W., and Zagaynov, V.: Particle size dependent response of aerosol counters, *Atmospheric Research*, 62, 209 – 237, [https://doi.org/https://doi.org/10.1016/S0169-8095\(02\)00011-X](https://doi.org/https://doi.org/10.1016/S0169-8095(02)00011-X), <http://www.sciencedirect.com/science/article/pii/S016980950200011X>, aerosol Number Concentration Measurement. International Workshop on Intercomparison of Condensation Nuclei and Aerosol Particle Counters, 2002.
- 5 Barmounis, K., Ranjithkumar, A., Schmidt-Ott, A., Attoui, M., and Biskos, G.: Enhancing the detection efficiency of condensation particle counters for sub-2nm particles, *Journal of Aerosol Science*, 117, 44 – 53, <https://doi.org/https://doi.org/10.1016/j.jaerosci.2017.12.005>, <http://www.sciencedirect.com/science/article/pii/S0021850217300216>, 2018.
- 10 Biskos, G., Malinowski, A., Russell, L. M., Buseck, P. R., and Martin, S. T.: Nanosize Effect on the Deliquescence and the Efflorescence of Sodium Chloride Particles, *Aerosol Science and Technology*, 40, 97–106, <https://doi.org/10.1080/02786820500484396>, <https://doi.org/10.1080/02786820500484396>, 2006.
- Castarède, D. and Thomson, E. S.: A thermodynamic description for the hygroscopic growth of atmospheric aerosol particles, *Atmospheric Chemistry and Physics*, 18, 14 939–14 948, <https://doi.org/10.5194/acp-18-14939-2018>, <https://www.atmos-chem-phys.net/18/14939/2018/>, 2018.
- 15 Chen, C.-C. and Tao, C.-J.: Condensation of supersaturated water vapor on submicrometer particles of SiO<sub>2</sub> and TiO<sub>2</sub>, *The Journal of Chemical Physics*, 112, 9967–9977, <https://doi.org/10.1063/1.481633>, <https://doi.org/10.1063/1.481633>, 2000.
- IPCC: Summary for Policymakers, book section SPM, pp. 1–30, Cambridge University Press, Cambridge, United Kingdom and New York, NY, USA, <https://doi.org/10.1017/CBO9781107415324.004>, [www.climatechange2013.org](http://www.climatechange2013.org), 2013.
- 20 Kaiser, J.: Mounting Evidence Indicts Fine-Particle Pollution, *Science*, 307, 1858–1861, <https://doi.org/10.1126/science.307.5717.1858a>, <http://science.sciencemag.org/content/307/5717/1858.1>, 2005.
- Kangasluoma, J., Samodurov, A., Attoui, M., Franchin, A., Junninen, H., Korhonen, F., Kurtén, T., Vehkamäki, H., Sipilä, M., Lehtipalo, K., Worsnop, D. R., Petäjä, T., and Kulmala, M.: Heterogeneous Nucleation onto Ions and Neutralized Ions: Insights into Sign-Preference, *The Journal of Physical Chemistry C*, 120, 7444–7450, <https://doi.org/10.1021/acs.jpcc.6b01779>, <https://doi.org/10.1021/acs.jpcc.6b01779>, 2016.
- 25 Krämer, L., Pöschl, U., and Niessner, R.: Microstructural rearrangement of sodium chloride condensation aerosol particles on interaction with water vapor, *Journal of Aerosol Science*, 31, 673 – 685, [https://doi.org/https://doi.org/10.1016/S0021-8502\(99\)00551-0](https://doi.org/https://doi.org/10.1016/S0021-8502(99)00551-0), <http://www.sciencedirect.com/science/article/pii/S0021850299005510>, 2000.
- 30 Kulmala, M., Lauri, A., Vehkamäki, H., Laaksonen, A., Petersen, D., and Wagner, P. E.: Strange Predictions by Binary Heterogeneous Nucleation Theory Compared with a Quantitative Experiment, *The Journal of Physical Chemistry B*, 105, 11 800–11 808, <https://doi.org/10.1021/jp011740c>, <https://doi.org/10.1021/jp011740c>, 2001.
- Kulmala, M., Petäjä, T., Ehn, M., Thornton, J., Sipilä, M., Worsnop, D., and Kerminen, V.-M.: Chemistry of Atmospheric Nucleation: On the Recent Advances on Precursor Characterization and Atmospheric Cluster Composition in Connection with Atmospheric New Particle Formation, *Annual Review of Physical Chemistry*, 65, 21–37, <https://doi.org/10.1146/annurev-physchem-040412-110014>, <https://doi.org/10.1146/annurev-physchem-040412-110014>, pMID: 24245904, 2014.
- 35



- Kupc, A., Winkler, P. M., Vrtala, A., and Wagner, P.: Unusual Temperature Dependence of Heterogeneous Nucleation of Water Vapor on Ag Particles, *Aerosol Science and Technology*, 47, i–iv, <https://doi.org/10.1080/02786826.2013.810330>, <https://doi.org/10.1080/02786826.2013.810330>, 2013.
- Li, C. and Christopher J. Hogan, J.: Vapor specific extents of uptake by nanometer scale charged particles, *Aerosol Science and Technology*, 51, 653–664, <https://doi.org/10.1080/02786826.2017.1288285>, <https://doi.org/10.1080/02786826.2017.1288285>, 2017.
- Loudon, M. G.: *Organic Chemistry*, 5 edn., 2009.
- Martin, S. T.: Phase Transitions of Aqueous Atmospheric Particles, *Chemical Reviews*, 100, 3403–3454, <https://doi.org/10.1021/cr990034t>, <https://doi.org/10.1021/cr990034t>, PMID: 11777428, 2000.
- McGraw, R., Wang, J., and Kuang, C.: Kinetics of Heterogeneous Nucleation in Supersaturated Vapor: Fundamental Limits to Neutral Particle Detection Revisited, *Aerosol Science and Technology*, 46, 1053–1064, <https://doi.org/10.1080/02786826.2012.687844>, <https://doi.org/10.1080/02786826.2012.687844>, 2012.
- McGraw, R. L., Winkler, P. M., and Wagner, P. E.: Temperature Dependence in Heterogeneous Nucleation with Application to the Direct Determination of Cluster Energy on Nearly Molecular Scale, *Scientific Reports*, 7, 2045–2322, <https://doi.org/10.1038/s41598-017-16692-9>, <https://doi.org/10.1038/s41598-017-16692-9>, 2017.
- McMurry, P. H.: A review of atmospheric aerosol measurements, *Atmospheric Environment*, 34, 1959 – 1999, [https://doi.org/https://doi.org/10.1016/S1352-2310\(99\)00455-0](https://doi.org/https://doi.org/10.1016/S1352-2310(99)00455-0), <http://www.sciencedirect.com/science/article/pii/S1352231099004550>, 2000.
- Merikanto, J., Spracklen, D. V., Mann, G. W., Pickering, S. J., and Carslaw, K. S.: Impact of nucleation on global CCN, *Atmospheric Chemistry and Physics*, 9, 8601–8616, <https://doi.org/10.5194/acp-9-8601-2009>, <https://www.atmos-chem-phys.net/9/8601/2009/>, 2009.
- Nel, A.: Air Pollution-Related Illness: Effects of Particles, *Science*, 308, 804–806, <https://doi.org/10.1126/science.1108752>, <http://science.sciencemag.org/content/308/5723/804>, 2005.
- Petersen, D., Ortner, R., Vrtala, A., Wagner, P. E., Kulmala, M., and Laaksonen, A.: Soluble-Insoluble Transition in Binary Heterogeneous Nucleation, *Phys. Rev. Lett.*, 87, 225 703, <https://doi.org/10.1103/PhysRevLett.87.225703>, <https://link.aps.org/doi/10.1103/PhysRevLett.87.225703>, 2001.
- Pope, C. A., Ezzati, M., and Dockery, D. W.: Fine-Particulate Air Pollution and Life Expectancy in the United States, *New England Journal of Medicine*, 360, 376–386, <https://doi.org/10.1056/NEJMsa0805646>, <https://doi.org/10.1056/NEJMsa0805646>, PMID: 19164188, 2009.
- Reichardt, C. and Welton, T.: *Solvents and Solvent Effects in Organic Chemistry*, Wiley-VCH Verlag GmbH & Co. KGaA, 4 edn., 2011.
- Saghafifar, H., Kürten, A., Curtius, J., von der Weiden, S.-L., Hassanzadeh, S., and Borrmann, S.: Characterization of a Modified Expansion Condensation Particle Counter for Detection of Nanometer-Sized Particles, *Aerosol Science and Technology*, 43, 767–780, <https://doi.org/10.1080/02786820902922894>, <https://doi.org/10.1080/02786820902922894>, 2009.
- Scheibel, H. and Porstendörfer, J.: Generation of monodisperse Ag- and NaCl-aerosols with particle diameters between 2 and 300 nm, *Journal of Aerosol Science*, 14, 113 – 126, [https://doi.org/https://doi.org/10.1016/0021-8502\(83\)90035-6](https://doi.org/https://doi.org/10.1016/0021-8502(83)90035-6), <http://www.sciencedirect.com/science/article/pii/0021850283900356>, 1983.
- Schobesberger, S., Winkler, P. M., Pinterich, T., Vrtala, A., Kulmala, M., and Wagner, P. E.: Experiments on the Temperature Dependence of Heterogeneous Nucleation on Nanometer-Sized NaCl and Ag Particles, *ChemPhysChem*, 11, 3874–3882, <https://doi.org/10.1002/cphc.201000417>, <https://onlinelibrary.wiley.com/doi/abs/10.1002/cphc.201000417>, 2010.
- Sem, G. J.: Design and performance characteristics of three continuous-flow condensation particle counters: a summary, *Atmospheric Research*, 62, 267 – 294, [https://doi.org/https://doi.org/10.1016/S0169-8095\(02\)00014-5](https://doi.org/https://doi.org/10.1016/S0169-8095(02)00014-5), <http://www.sciencedirect.com/science/article/pii/S0169809502000145>, 2002.



- S0169809502000145, aerosol Number Concentration Measurement. International Workshop on Intercomparison of Condensation Nuclei and Aerosol Particle Counters, 2002.
- Soysal, U., Géhin, E., Algré, E., Berthelot, B., Da, G., and Robine, E.: Aerosol mass concentration measurements: Recent advancements of real-time nano/micro systems, *Journal of Aerosol Science*, 114, 42 – 54, <https://doi.org/https://doi.org/10.1016/j.jaerosci.2017.09.008>,  
5 <http://www.sciencedirect.com/science/article/pii/S0021850216303998>, 2017.
- Spracklen, D. V., Carslaw, K. S., Kulmala, M., Kerminen, V.-M., Sihto, S.-L., Riipinen, I., Merikanto, J., Mann, G. W., Chipperfield, M. P., Wiedensohler, A., Birmili, W., and Lihavainen, H.: Contribution of particle formation to global cloud condensation nuclei concentrations, *Geophysical Research Letters*, 35, <https://doi.org/10.1029/2007GL033038>, <http://dx.doi.org/10.1029/2007GL033038>, 106808, 2008.
- Tauber, C., Chen, X., Wagner, P. E., Winkler, P. M., Hogan, C. J., and Maisser, A.: Heterogeneous Nucleation onto Monoatomic Ions: Support for the Kelvin-Thomson Theory, *ChemPhysChem*, 19, 3144–3149, <https://doi.org/10.1002/cphc.201800698>, <https://onlinelibrary.wiley.com/doi/abs/10.1002/cphc.201800698>, 2018.
- Tauber, C., Steiner, G., and Winkler, P. M.: Counting Efficiency Determination from Quantitative Intercomparison between Expansion and Laminar Flow Type Condensation Particle Counter, *Aerosol Science and Technology*, 0, 1–11, <https://doi.org/10.1080/02786826.2019.1568382>, <https://doi.org/10.1080/02786826.2019.1568382>, 2019.
- 15 Thomson, S. W.: On the equilibrium of vapour at a curved surface of liquid, *Philosophical Magazine*, 42, 448–452, 1871.
- Wagner, P.: A constant-angle mie scattering method (cams) for investigation of particle formation processes, *Journal of Colloid and Interface Science*, 105, 456 – 467, [https://doi.org/https://doi.org/10.1016/0021-9797\(85\)90319-4](https://doi.org/https://doi.org/10.1016/0021-9797(85)90319-4), <http://www.sciencedirect.com/science/article/pii/0021979785903194>, 1985.
- Wagner, P. E., Kaller, D., Vrtala, A., Lauri, A., Kulmala, M., and Laaksonen, A.: Nucleation probability in binary heterogeneous nucleation of water–n-propanol vapor mixtures on insoluble and soluble nanoparticles, *Phys. Rev. E*, 67, 021605, <https://doi.org/10.1103/PhysRevE.67.021605>, <https://link.aps.org/doi/10.1103/PhysRevE.67.021605>, 2003.
- 20 Wang, J., McGraw, R. L., and Kuang, C.: Growth of atmospheric nano-particles by heterogeneous nucleation of organic vapor, *Atmospheric Chemistry and Physics*, 13, 6523–6531, <https://doi.org/10.5194/acp-13-6523-2013>, <https://www.atmos-chem-phys.net/13/6523/2013/>, 2013.
- 25 Wiedensohler, A., Orsini, D., Covert, D. S., Coffmann, D., Cantrell, W., Havlicek, M., Brechtel, F. J., Russell, L. M., Weber, R. J., Gras, J., Hudson, J. G., and Litchy, M.: Intercomparison Study of the Size-Dependent Counting Efficiency of 26 Condensation Particle Counters, *Aerosol Science and Technology*, 27, 224–242, <https://doi.org/10.1080/02786829708965469>, <https://doi.org/10.1080/02786829708965469>, 1997.
- Winkler, P. M., Hienola, A., Steiner, G., Hill, G., Vrtala, A., Reischl, G. P., Kulmala, M., and Wagner, P. E.: Effects of seed particle size and composition on heterogeneous nucleation of n-nonane, *Atmospheric Research*, 90, 187 – 194, <https://doi.org/https://doi.org/10.1016/j.atmosres.2008.02.001>, <http://www.sciencedirect.com/science/article/pii/S016980950800032X>, 17th International Conference on Nucleation and Atmospheric Aerosols, 2008.
- 30 Winkler, P. M., McGraw, R. L., Bauer, P. S., Rentenberger, C., and Wagner, P. E.: Direct determination of three-phase contact line properties on nearly molecular scale, *Scientific Reports*, 6, 26 111, <https://doi.org/10.1038/srep26111>, <http://dx.doi.org/10.1038/srep26111>, 2016.